Canadian Conference - Pacific Conference on Earthquake Engineering 2023

Vancouver, British Columbia

June 25th – June 30th, 2023

Numerical Framework to Evaluate Liquefaction-Induced Pipe Uplift

Devdeep Basu[1*], Dharma Wijewickreme[2]

[1]Postdoctoral Research Fellow, Department of Civil Engineering, University of British Columbia, Vancouver, BC, Canada
[2]Professor, Department of Civil Engineering, University of British Columbia, Vancouver, BC, Canada
[*]devdeep.basu@ubc.ca (Corresponding Author)

ABSTRACT

Soil liquefaction is an important phenomenon in geotechnical engineering that poses severe risk to both above-ground and buried structures. Pipelines play an essential role in the safe transmission of fluids (e.g., water, oil, and gas) over large distances; as such, their integrity under operating conditions and seismic shaking is a key concern for the industry as well as the public. Uplift of buried structures and pipelines due to liquefaction of soils have been reported during earthquakes in the past. This study aims to numerically investigate the uplift response of buried pipelines in potentially liquefiable soils under the event of seismic loading. A numerical framework is developed using the numerical platform FLAC and the constitutive model PM4Sand to model the response of shallow-buried pipes; Fraser River sand, a material that has been studied extensively and found abundantly in the Lower Mainland region of British Columbia, Canada, is considered as the soil material for the model. Two dimensional models representing several buried pipe configurations, subjected to harmonic input ground motions having different acceleration amplitudes are analyzed. The observed effects of input motion intensity and pipe diameter on uplift magnitude are investigated. The corresponding excess pore pressure and ground displacement patterns are also presented.

Keywords: soil liquefaction, pipelines, uplift, earthquake shaking, numerical modeling.

INTRODUCTION

Earthquake-induced soil liquefaction is a critical phenomenon that poses vulnerability to not only above-ground infrastructure but also to buried structures. During liquefaction, the shear strength of the soil above and around the buried structure could decrease due to build-up of excess pore pressures and, subsequently, resulting in buoyancy forces that could cause the structure to displace and potentially "float up" towards the ground surface. Liquefaction-induced uplift of underground structures have been reported during past seismic events such as the 1964 Niigata earthquake [1], the 1989 Loma Prieta earthquake [2], and the 2010 Chile earthquake [3], to name a few. Buried pipelines are essential for safe transportation of fluids over long distances, and therefore, pipeline integrity under static or seismic loading is a key concern as rehabilitation of damaged pipelines require a considerable amount of time and expense. The characterization of soil restraints developed during relative ground movements due to landslides, lateral spreads or fault movements (in the form of numerical force-displacement "soil springs") in lateral, vertical, oblique or axial directions have been widely studied [4, 5, 6] and guidelines have been developed for engineering practice [7]. Liquefaction-induced uplift of manholes, tunnels and large-diameter pipes buried in saturated soil has been investigated utilizing experiments as well as numerical models [8-10]. However, there are very few limited studies characterizing the uplift response of buried pipelines in liquefied soils [11, 12]. It is common practice to utilize force equilibrium equations to estimate the factor of safety against uplift as described by Koseki et al. [8] to evaluate the stability of buried pipelines. However, such limit equilibrium based analytical procedures only provide the uplift triggering conditions and forces but predicting the magnitude of uplift displacements is a complex task with a number of soil (relative density, friction angle etc.), pipe (burial depth and diameter) and seismic (peak ground acceleration, Arias intensity etc.) parameters contributing to the associated physical mechanism. Yasuda et al. [14] and Saeedzadeh and Hataf [10] performed shake table tests and numerical simulations, respectively, to establish trends between uplift magnitude and various soil and pipe parameters. However, the physical mechanism of soil-pipe interaction would depend on regional soil properties, and therefore, design of new pipelines should be based on site-specific evaluation of pipe uplift.

In this study, pipe uplift characteristics and associated soil response for pipelines buried in Fraser River Sand (FRS) were numerically investigated. FRS is abundantly found in the Fraser River Delta and Fraser Valley of the Lower Mainland region of British Columbia, Canada through which several water and natural gas pipelines traverse. Since situated in a seismically active zone associated with a subduction zone, the saturated loose soils in this region have a considerably high liquefaction potential [15] (categorized as Seismic Zone 4 as per NBC [16]). A well-calibrated numerical framework was established and validated with respect to the results from a centrifuge test on liquefaction-induced pipe uplift [19]. Thereafter, the numerical framework was used to estimate the uplift for shallow-buried pipes of two different diameters buried in a saturated, loose, and uniform deposit of FRS. Harmonic excitations were utilized in the numerical simulations. The main objective of this study was to evaluate the effect of shaking intensity and pipe diameter on uplift magnitude, while assessing the associated soil responses such as excess pore pressure development and ground displacement. This study provides initial input to frameworks assessing the risk due to liquefaction-induced uplift for existing pipelines as well as design of new pipelines.

NUMERICAL MODELING

Simulation approach

The constitutive model PM4Sand v3.1 [18] emloyed on commercially available FLAC v8.1 [19] finite difference software was used in the numerical analysis. The boundary value problem comprised a finite difference mesh having a width of 18 m and a thickness of 12 m (Figure 1) that was used to represent a uniform deposit of FRS with a steel pipe having a diameter (*D*) and burial depth (*H*) assumed to be buried in the deposit. The finite difference mesh consisted of square zones with a dimension of 0.2 m by 0.2 m; this mesh size was able to propagate all frequencies below 87 Hz [20] and it was chosen by optimizing the solution time and accuracy for each simulation. As shown in Figure 1, additional soil columns were also used over a separation distance (*W*) of 80 m on either sides of the 18 m region-of-interest (ROI); the intent herein was to represent a field scenario of semi-infinite soil deposit and isolate the ROI from any lateral boundary effects such as wave reflections that would take place when smaller mesh sizes are used. The pipe was modeled using 32 elastic beam elements and assuming the following material properties for steel - density = 7850 kg/m^3 and Young's modulus = 200 GPa. The pipe wall thicknesses utilized varied between 5 to 10 mm depending on the pipe diameter in accordance with CSA Z662-19 [13]. The pipe-soil contact was modeled using unbonded interfaces to simulate a frictional interface between the two materials with separation and slippage permitted. The soil properties assumed for FRS are given in Table 1. A soil-pipe interface friction angle (δ) of 23° (2/3rd of φ'_{cv}) was used, similar to that used by Chain et al. [21] used in a similar pipe uplift study. The normal and shear stiffnesses for the interface were set to 3.1 GPa, which was approximately equal to 10 times the stiffness of the neighboring soil, as recommended in the FLAC User Manual [19]. The default timestep used for each simulation was calculated internally by FLAC as the largest timestep that it could use while maintaining solution stability.

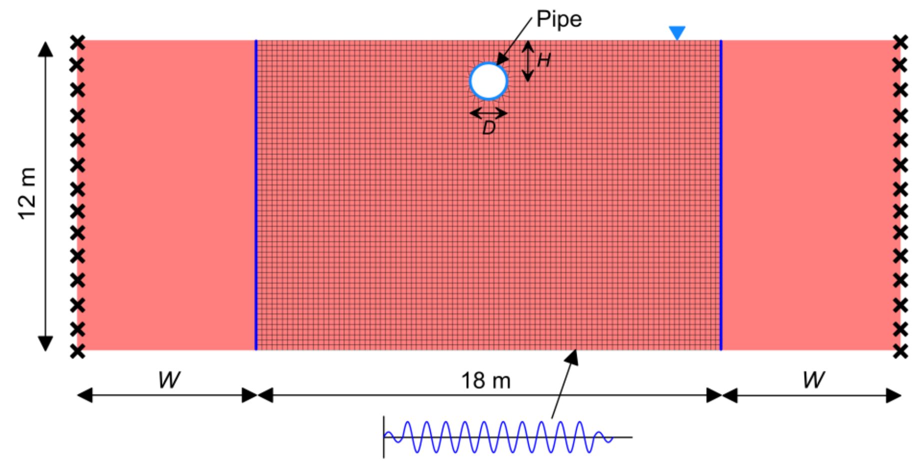

Figure 1. Numerical model of the FRS deposit with a buried pipe simulated in FLAC.

There were two stages in each simulation. In the first stage, the model geometry, soil properties, and boundary conditions were defined, and the geostatic stress state (static equilibrium) was achieved by simulating gravity. Hydrostatic pore pressure conditions were established across the model to match the depth of the ground water table which was assumed to be at the ground surface. The base of the model was fixed against movement. Only vertical movements along the sides of the model were allowed in both stages – commonly used lateral boundary condition when simulating soil deposits. In the second stage of the analysis, earthquake shaking was applied to the base of the model as a horizontal acceleration time history. Drainage could take place from the model top, but the sides of the model were considered as no flow boundaries for both stages. To mitigate numerical noise, a Rayleigh damping of 0.5% centered at the predominant frequency of the soil deposit was used based on recommendations by Boulanger and Ziotopoulou [18].

PM4Sand calibration

The nonlinear constitutive model PM4Sand v3.1 [18] was used for the simulations described herein. PM4Sand requires three primary input parameters, 21 secondary parameters, the atmospheric pressure (P_a) which sets the units, and two flag variables. The three primary parameters must be calibrated to the specific soil type being modeled, whereas all secondary parameters have been pre-calibrated by the developers to a broader body of clean sand data to reasonably approximate the general range of sand behavior. The primary PM4Sand parameters relative density (D_r), shear modulus coefficient (G_o), and contraction rate parameter (h_{po}) were calibrated in this study. D_r controls the relative state of soil and thus its contractive or dilative behavior, G_o is related to the shear wave velocity (V_s) and controls the small-strain shear stiffness (G_{max}). The parameter h_{po} controls the contractiveness of the soil material and, therefore, its cyclic strength. The maximum void ratio (e_{max}), minimum void ratio (e_{min}), and critical state friction angle (φ'_{cv}) were assigned values based on relevant FRS data [24-27]. Default values of all the other PM4Sand parameters as described in Boulanger and Ziotopoulou [18] were used.

For the current study, a D_r value of 40% was used for all the simulations to evaluate liquefaction-induced uplift in a relatively loose deposit. Equations 1 and 2 were used to estimate G_o for a range of D_r (Figure 2a) wherein the shear wave velocity measurements reported by Chillarige et al. [24] were utilized. G_o estimated from bender element test results by Naesgaard [28] is also plotted in Figure 2a alongside the default PM4Sand correlation for G_o [18].

$$G_{max} = \rho V_s^2 \tag{1}$$

$$G_o = \frac{G_{max}}{P_a}\left(\frac{P_a}{p'}\right)^{0.5} \tag{2}$$

where, ρ is the soil density, and p' is the mean effective confining pressure. Laboratory data on liquefaction triggering was available for FRS [29] at a D_r of 40% and was used to calibrate h_{po}. This calibration was performed using single element cyclic direct simple shear (DSS) simulations to approximately match the cyclic resistance ratio to reach 3% single amplitude shear strain in 15 cycles (Figure 2b). Table 1 outlines the key PM4Sand calibration parameters and soil properties used in this study.

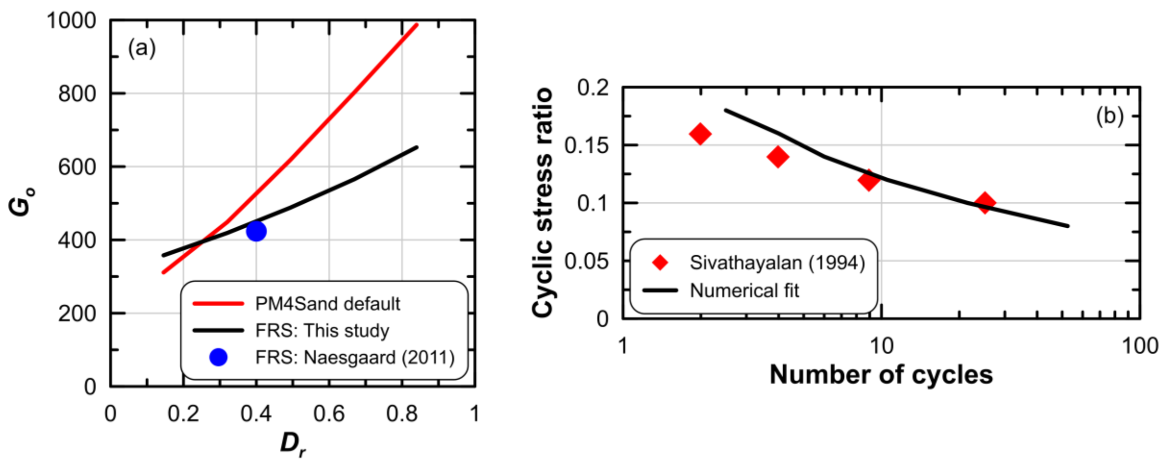

Figure 2. (a) Shear modulus coefficient vs relative density correlation used for this study; and (b) laboratory DSS test results on FRS from Sivathayalan [29] and calibrated DSS simulations at a confinement of 100 kPa.

Table 1. PM4Sand calibration parameters and FRS properties.

D_r (%)	G_o	h_{po}	k[1] (cm/s)	G_s[2]	e_{max}	e_{min}	φ'_{cv}
40	457	0.7	0.042	2.71	0.95	0.62	35°

[1] Hydraulic conductivity, k based on Tsaparli et al. [30].
[2] Specific gravity of solids, G_s based on Northcutt and Wijewickreme [31].

Input motion

Harmonic motions having peak ground accelerations (PGAs) of 0.15g, 0.3g, and 0.6g were used for the simulations. Each of these motions have a duration of 12 s and a frequency of 1 Hz with the first and last cycles having an amplitude equal to 1/3rd of the peak acceleration as shown in Figure 3. The choice of such regular ground motion time histories, instead of irregular real-life ground motions, for these types of simulations are in accordance with previous studies [10, 21].

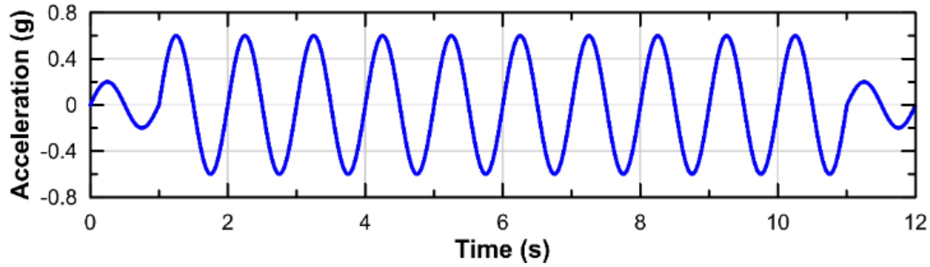

Figure 3. A typical acceleration-time history applied as input motion in the numerical simulations.

VALIDATION STUDY

The numerical framework calibrated as described in the previous section was validated by simulating the centrifuge experiment (referred to as PLM2) performed by Sun [19]. The centrifuge test had been performed on a loose, uniform, and homogeneous deposit of Nevada sand having the same D_r of 40% as considered for the simulations on FRS in the current study. The sand deposit had a width of 21 m and a thickness of 9 m in prototype units. An aluminum alloy pipe having a D of 3 m was buried at a depth (H) of 4.5 m in the deposit. A harmonic motion having a frequency of 3 Hz, duration of 60 s and an amplitude of 0.3g was applied at the base of the model. The index properties of Nevada sand considered in the simulation were used as those described by Arulmoli [32]: G_o was calculated as 710 based on resonant column test data by Arulmoli [32] and h_{po} was determined as 0.45 based on calibration performed with respect to liquefaction strength curves on Nevada sand [32, 33]. A W of 80 m was used for the simulation to minimize lateral boundary effects as described earlier.

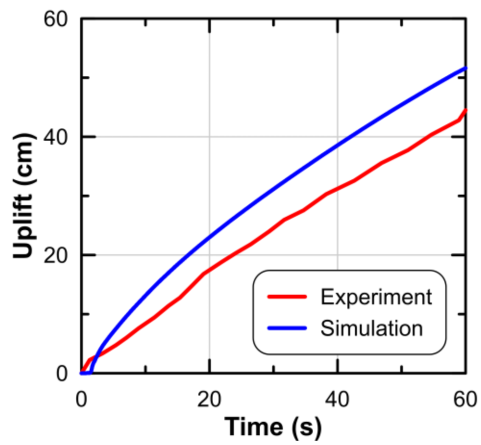

Figure 4. Uplift time histories predicted by the simulation and observed for the centrifuge experiment.

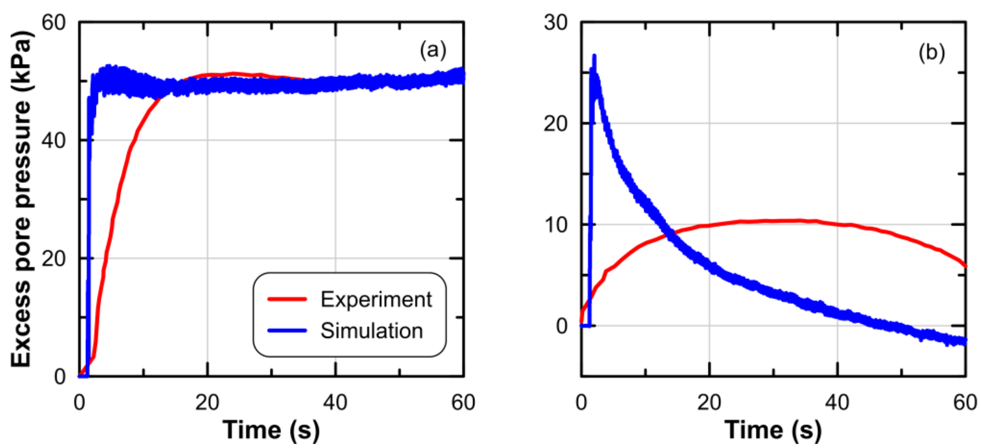

Figure 5. Excess pore pressure time histories observed for the experiment and predicted by the simulation at (a) invert and (b) crown of the pipe.

Figure 4 shows the uplift predicted by the numerical simulation compared to the uplift observed for the centrifuge test. The rate of uplift is similar between the simulation and experiment. However, the uplift magnitude at the end of shaking is overpredicted by 16%. This level of uncertainty is considerably smaller than the 50-200% range commonly deemed as acceptable in liquefaction studies [34-37]. The excess pore pressure predicted at the end of shaking at the pipe invert is similar to that observed for the experiment (Figure 5a) while the end-of-shaking excess pore pressure at the crown of the pipe is underpredicted (Figure 5b). It is to be noted that, since the digital data was not available, the results from the experiments was digitized from a hardcopy of the publication by Sun [19]; as such, the excess pore pressure time histories presented in Figure 5 for the experiment only represent the trend, as it was challenging to digitize the small spikes that were observed throughout the duration of shaking. The rate of excess pore pressure generation is different between the simulation and the experiment. These discrepancies may be attributed to experimental factors such as movement of pore pressure sensors during testing, variation in D_r achieved across the deposit, or inability of the 2D numerical model used herein to capture the pore pressure migration in the radial direction that may have occurred in the experiment. Since the major focus of this study was to assess pipe uplift, the numerical framework was deemed suitable.

RESULTS

This section outlines some of the soil and pipe responses for two sets of simulations considering FRS. The first set considered a large size pipe having a D of 1.5 m, and the second case considered a D of 0.9 m with the H being 1.6 m for both. This resulted in approximate H/D ratios of 1.1 and 1.8, respectively, for the two cases; these cases are considered representative of typical shallow-buried gas pipelines in the field. Each set was subjected to harmonic motions with three different amplitudes as described earlier. The pipe uplift, excess pore pressure ratio (r_u), defined as the ratio of excess pore pressure and vertical effective stress, and ground surface displacement were investigated.

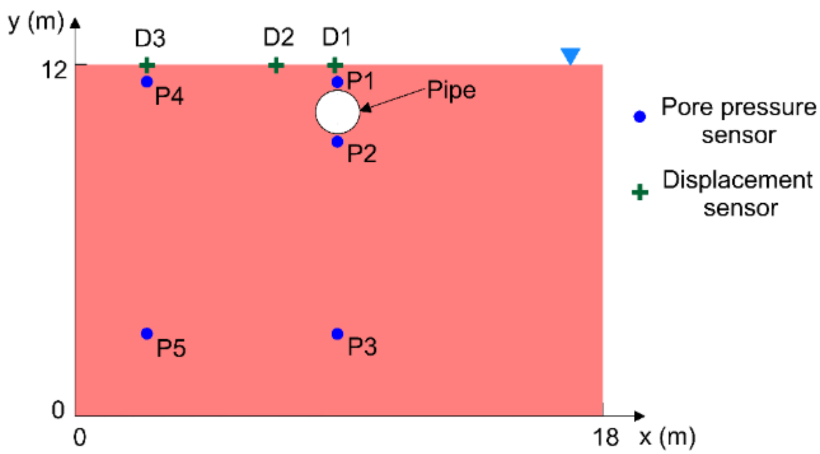

Figure 6. Locations where pore water pressure and displacements were computed in the FLAC model.

Figure 6 outlines the location where the development of pore water pressure and displacement were computed in the numerical simulations. The displacements are computed at selected locations D1, D2, and D3 on the ground surface, where they correspond with the vertical axis of the pipe, and 2 m and 7 m away from the vertical axis, respectively. The pore pressures were computed at: (i) the crown and invert locations of the pipe (locations P1 and P2 respectively); and three far-field locations of P3 (along the vertical axis of pipe at a depth of 10 m), P4 (7 m away from the vertical axis near the ground surface), and P5 (7 m away from the vertical axis at a depth of 10 m) as shown in Figure 6.

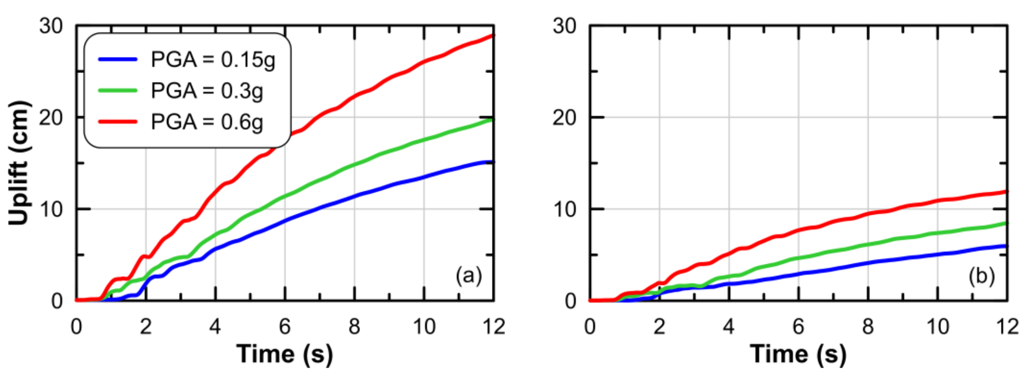

Figure 7. Uplift time histories for the simulations with: (a) D = 1.5 m; and (b) D = 0.9 m.

Figure 7 shows the uplift time histories obtained for both sets of simulations. The end-of-shaking uplift magnitude was higher for the case with larger diameter pipe for all the shaking intensities; these results are in accordance with those noted in the study by Yasuda et al. [14]. For both pipe diameters, the end-of-shaking uplift increased with increasing PGA; as PGA increased from 0.15g to 0.6g, uplift increased from 15.1 to 28.9 cm (91% increase) for the first simulation set with D = 1.5 m, and the variation was from 6.0 to 11.9 cm (98% increase) for the second simulation set corresponding to D = 0.9 m.

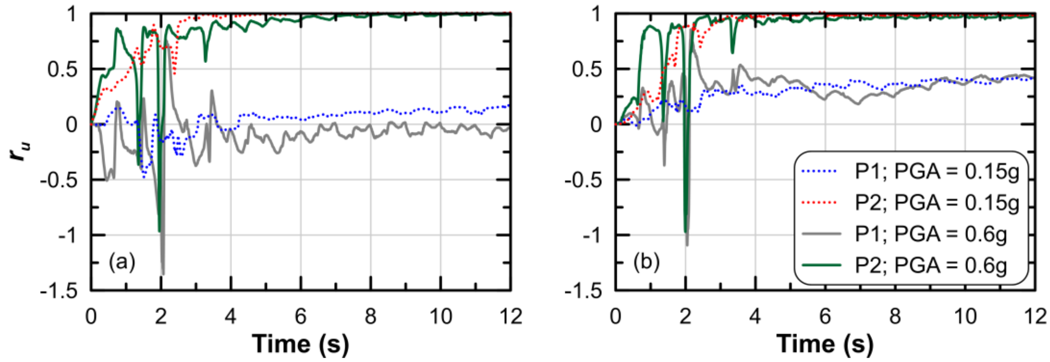

Figure 8. r_u time histories at the crown and invert of pipe for the simulation sets: (a) D = 1.5 m; (b) D = 0.9 m.

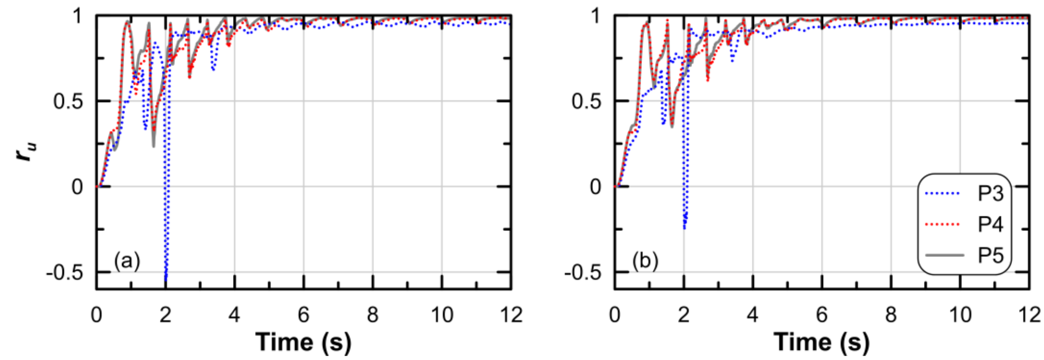

Figure 9. r_u time histories in the far-field using PGA = 0.6g motion for the simulations conducted with: (a) D = 1.5 m; and (b) D = 0.9 m.

A significant difference in r_u above (crown) and below (invert) the pipe was observed (Figure 8) for all the simulations as also noted in past experimental and numerical studies on liquefaction-induced pipe uplift [12, 21]. For both simulation sets, initial liquefaction ($r_u \sim 1$) was observed at the pipe invert and strong dilation spikes around 2 s were observed both at the crown and invert in case of the higher PGA = 0.6g motion. Such dilation spikes had also been reported by Ecemis et al. [12] in their shake table study on liquefaction-induced pipe uplift. At the crown of the pipe, relatively low r_u values at the end-of-shaking of about 0.4 were observed for the simulations using D = 0.9 m (Figure 8b); this end-of-shaking r_u values were noted to be further low for the case with D to 1.5 m (Figure 8a). Figure 9 shows the r_u observed at points P3, P4, and P5 located significantly away from the pipe for the simulations using the input motion with a PGA of 0.6g. Initial liquefaction was observed at all locations P3, P4, and P5. A sharp dilation spike was observed at about 2 s at the point P3, located at a depth of 10 m below the ground surface and below the pipe invert.

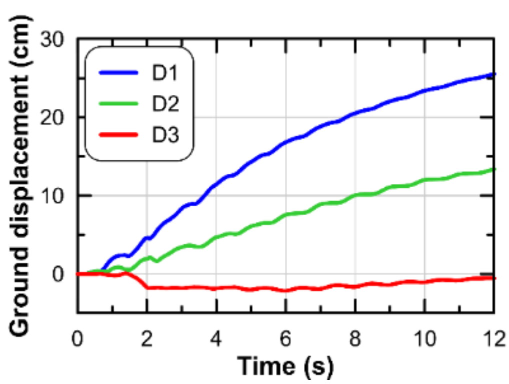

Figure 10. Ground displacement observed for the simulation having a D of 1.5 m using the PGA = 0.6g input motion.

Figure 10 shows the ground displacement observed at the locations D1, D2, and D3 for the simulation having a D of 1.5 m using the PGA = 0.6g motion. A significant ground upheaval was observed at sensor D1 above the pipe, and this upward displacement decreased with increasing horizontal distance from the vertical through the centerline of pipe - with no heave observed beyond a distance of 7 m from the vertical axis of the pipe. This observation is similar to ground displacement patterns reported in past studies on liquefaction-induced uplift of hollow underground structures [38, 39].

CONCLUSIONS

In this study, the uplift characteristics and associated soil response for two pipe diameters buried in potentially liquefiable soils were investigated under seismic loading. A numerical model was developed using the commercially available FLAC software and PM4Sand constitutive model; the modeling approach was validated with respect to a data set available from a centrifuge test on liquefaction-induced pipe uplift. The constitutive model was calibrated to characterize the cyclic behavior of Fraser River sand which is found abundantly in the lower mainland region of British Columbia. Thereafter, the numerical model was used to estimate the uplift for shallow-buried (burial depth, H of 1.6 m) pipes of two different diameters (D) of 1.5 and 0.9 m buried in a saturated, loose, and uniform deposit of Fraser River sand. Harmonic input motions having peak ground accelerations (PGAs) of 0.15g, 0.3g and 0.6g were used. Some of the key observations from this study were:

- The end-of-shaking pipe uplift magnitude was higher for the case with larger diameter pipe for all the shaking intensities.
- For both simulation sets using two different D, the end-of-shaking uplift magnitude increased by about a factor of 2 as the input motion PGA increased from 0.15g to 0.6g.
- The excess pore pressure ratio (r_u) varied considerably between the crown and invert of the pipe with initial liquefaction observed at the invert but r_u values were much lower at the crown.
- Significant ground heave was observed above the pipe and the magnitude of heave decreased farther away from the vertical axis of the pipe with no observed ground heaving beyond a distance of 7 m from the pipe vertical axis.

This study provides some insights to assess the risk due to liquefaction-induced uplift for existing pipelines. Additional work needs to be undertaken in this domain by considering a wider range of pipe diameter and burial depth combinations, as well as input motion characteristics to further the knowledge on liquefaction-induced uplift potential of Fraser River sand.

ACKNOWLEDGMENTS

The support provided by the Pipeline Integrity Institute at the University of British Columbia (UBC-PII), originating from the sponsorships provided by pipeline industry partners, is deeply appreciated.

REFERENCES

[1] Okamoto, S. (1984). *Introduction to earthquake engineering*. Second edition, University of Tokyo Press.
[2] O'Rourke, T.D., and Lane, P.A. (1989). *Liquefaction hazards and their effects on buried pipelines*. Rep. No. NCEER-89-0007.
[3] Association GEERG. (2010). *Geoengineering reconnaissance of the 2010 Maule, Chile earthquake*. Report of the NSF Sponsored GEER Association Team.
[4] Trautmann, C.H., and O'Rourke, T.D. (1985). "Lateral force displacement response of buried pipe". *Journal of Geotechnical Engineering*, 111 (9), 1077-1092.
[5] Wijewickreme, D., Karimian, H., and Honegger, D. (2009). "Response of buried steel pipelines subjected to relative axial soil movement". *Canadian Geotechnical Journal*, 46, 735-752.
[6] Wijewickreme, D., Monroy, M., Honegger, D.G., and Nyman, D.J. (2017). "Soil restraints on buried pipelines subjected to reverse-fault displacement". *Canadian Geotechnical Journal*, 54, 1472-1481.
[7] Pipeline Research Council International. (2009). *Guidelines for Natural Gas and Liquid Hydrocarbon Pipelines in Areas Prone to Landslide and Subsidence Hazards*. Report prepared by C-CORE, D.G. Honegger Consulting, and SSD, Inc., Catalog No. L52292.
[8] Koseki, J., Matsuo, O., Ninomiya, Y., and Yoshida, T. (1997). "Uplift of Sewer Manholes During The 1993 Kushiro-Oki Earthquake". *Soils and Foundations*, 37, 109-121.
[9] Ling, H.I., Mohri, Y., Kawabata, T., Liu, H., Burke, C., and Sun, L. (2003). "Centrifugal Modeling of Seismic Behavior of Large-Diameter Pipe in Liquefiable Soil". *Journal of Geotechnical and Geoenvironmental Engineering*, 129, 1092-1101.
[10] Saeedzadeh, R., and Hataf, N. (2011). "Uplift response of buried pipelines in saturated sand deposit under earthquake loading". *Soil Dynamics and Earthquake Engineering*, 31, 1378-1384.
[11] Castiglia, M., Santucci de Magistris, F., Onori, F., and Koseki, J. (2021) "Mitigation systems for the uplift of buried pipelines in liquefiable soils under repeated shaking through model tests". *Soil Dynamics and Earthquake Engineering*, 148, 106850.

[12] Ecemis, N., Valizadeh, H., and Karaman, M. (2021) "Sand-granulated rubber mixture to prevent liquefaction-induced uplift of buried pipes: a shaking table study". *Bulletin of Earthquake Engineering*, 19, 2817-2838.
[13] Z662:19 C. (2019*). Oil and gas pipeline systems*. pp. 917.
[14] Yasuda, S., Nagase, H., Itafuji, S., Sawada, H., and Mine, K. (1995). "A study on the mechanism of the floatation of buried pipes due to liquefaction". *WIT Transactions on The Built Environment*, 15, 1-8.
[15] Clague, J.J., Luternauer, J.L., and Mosher, D.C. (1998). *Geology and natural hazards of the Fraser River Delta, British Columbia*. Geological Survey of Canada Bulletin 525, pp. 270.
[16] Canadian Commission on B, Fire C. (2022). *National Building Code of Canada: 2020*.
[17] Itasca. (2016). *FLAC (Version 8.0) – Fast Lagrangian Analysis of Continua*.
[18] Boulanger, R., and Ziotopoulou, K. (2017). *PM4Sand (Version 3.1): A sand plasticity model for earthquake engineering applications*. Report No. UCD/CGM-17/01, Davis, CA: University of California, Davis.
[19] Sun, L. (2001). "Centrifuge Modeling and Finite Element Analysis of Pipeline Buried in Liquefiable Soil". *Ph.D thesis*, Columbia University.
[20] Kuhlemeyer, R.L., and Lysmer, J. (1973). "Finite Element Method Accuracy for Wave Propagation Problems". *Journal of the Soil Mechanics and Foundations Division*, 99, 421-427.
[21] Chian, S.C., Tokimatsu, K., and Madabhushi, S.P.G. (2014). "Soil liquefaction–induced uplift of underground structures: physical and numerical modeling". *Journal of Geotechnical and Geoenvironmental Engineering*, 140, 04014057.
[22] Pretell, R., Ziotopoulou, K., and Abrahamson, N.A. (2022). "Conducting 1D site response analyses to capture 2D VS spatial variability effects". *Earthquake Spectra*, 38, 87552930211069400.
[23] Azadi, M., and Mir Mohammad Hosseini, S.M. (2010). "The uplifting behavior of shallow tunnels within the liquefiable soils under cyclic loadings". *Tunnelling and Underground Space Technology*, 25, 158-167.
[24] Chillarige, A.V., Robertson, P.K., Morgenstern, N.R., and Christian, H.A. (1997). "Evaluation of the in situ state of Fraser River sand". *Canadian Geotechnical Journal*, 34, 510-519.
[25] Sivathayalan, S., and Vaid, Y.P. (2002). "Influence of generalized initial state and principal stress rotation on the undrained response of sands". *Canadian Geotechnical Journal*, 39, 63-76.
[26] Wijewickreme, D., Sriskandakumar, S., and Byrne, P.M. (2005). "Cyclic Loading Response of Loose Air-pluviated Fraser River Sand for Validation of Numerical Models Simulating Centrifuge Tests", *Canadian Geotechnical Journal*, 42 (2), 550-561.
[27] Dabeet, A.E. (2008). "A practical model for load-unload-reload cycles on sand". *Masters' thesis*, Department of Civil Engineering, The University of British Columbia.
[28] Naesgaard, E. (2011). "A hybrid effective stress - total stress procedure for analyzing soil embankments subjected to potential liquefaction and flow". *Ph.D thesis*, Department of Civil Engineering, The University of British Columbia.
[29] Sivathayalan, S. (1994). "Static, cyclic and post liquefaction simple shear response of sands". *Masters' thesis*, Department of Civil Engineering, The University of British Columbia.
[30] Tsaparli, V., Kontoe, S., Taborda, D.M.G., and Potts, D.M. (2017). "An energy-based interpretation of sand liquefaction due to vertical ground motion". *Computers and Geotechnics*, 90, 1-13.
[31] Northcutt, S., and Wijewickreme, D. (2013). "Effect of particle fabric on the coefficient of lateral earth pressure observed during one-dimensional compression of sand". *Canadian Geotechnical Journal*, 50, 457-466.
[32] Arulmoli, K., Muraleetharan, K.K., Hossain, M.M., and Fruth, L.S. (1992). *VELACS Soil Data Report*.
[33] Doygun, O. (2009). "Monotonic and cyclic undrained loading behavior of intermediate soils". *M.Sc. dissertation*, Technische University.
[34] Bartlett, S.F., and Youd, T.L. (1995). "Empirical Prediction of Liquefaction-Induced Lateral Spread". *Journal of Geotechnical Engineering*, 121, 316-329.
[35] Geyin, M., and Maurer, B.W. (2019). "An Analysis of Liquefaction-Induced Free-Field Ground Settlement Using 1,000+ Case Histories: Observations vs. State-of-Practice Predictionsz". In: *Geo-Congress*, p. 489-498.
[36] Basu, D., Montgomery, J., and Stuedlein, A.W. (2022). "Observations and challenges in simulating post-liquefaction settlements from centrifuge and shake table tests". *Soil Dynamics and Earthquake Engineering*, 153, 107089.
[37] Basu, D., Pretell, R., Montgomery, J., and Ziotopoulou, K. (2022). "Investigation of key parameters and issues in simulating centrifuge model tests of a sheet-pile wall retaining a liquefiable soil deposit". *Soil Dynamics and Earthquake Engineering*, 156, 107243.
[38] Khoshnoudian, F., and Shahrour, I. (2002). "Numerical Analysis of the Seismic Behavior of Tunnels Constructed in Liquefiable Soils". *Soils and Foundations*, 42, 1-8.
[39] Liu, H., and Song, E. (2005). "Seismic response of large underground structures in liquefiable soils subjected to horizontal and vertical earthquake excitations". *Computers and Geotechnics*, 32, 223-244.